

SLAC-PUB-539
HEPL-593
January 1969
(EXP)

PHOTODISINTEGRATION OF THE DEUTERON FROM 220 MeV to 340 MeV*

by

R. L. Anderson, R. Prepost[†]
Stanford Linear Accelerator Center
Stanford University, Stanford, California

and

B. H. Wiik^{††}
High Energy Physics Laboratory
Stanford University, Stanford, California

ABSTRACT

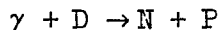
The differential cross-section for the photodisintegration of the deuteron has been measured at laboratory photon energies of 222, 254, 302, 342 MeV in CM angle steps of 10° between 20° CM and 160° CM.

* Work supported in part by the U. S. Office of Naval Research Contract (Nonr 225 (67)) and in part by the U. S. Atomic Energy Commission.

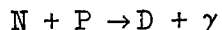
[†] Permanent Address: University of Wisconsin, Madison, Wisconsin.

^{††} Present Address: Stanford Linear Accelerator Center, Stanford, California.

Recent speculations^(1,2) have made it very desirable to check experimentally CP or T invariance in the electromagnetic interactions of the hadrons. One possible test⁽³⁾ of T invariance is to compare the reaction



with the time reversed reaction



in the region around the first resonance. The reciprocity check in this energy region could be sensitive to a breakdown of time reversal invariance in the γNN^* vertex. The most sensitive reciprocity test would presumably be a comparison of the angular distributions of the two reactions.

The capture reaction is presently being studied by several groups which are in the process of reducing their data. The photodisintegration differential cross-section in this energy region has been measured by several groups.^(4,5,6) The agreement between the two most recent photodisintegration measurements is good at forward angles but there is a definite disagreement at backward angles, and the experiments contain only 6 to 7 points for each angular distribution. We report here measurements in 10° steps between 20° CM and 160° CM at 4 energies from 222 MeV to 340 MeV.

The experiment was carried out using the Stanford Mark III Linear Accelerator. The momentum analyzed electron beam ($\Delta E/E = .5\%$) was focussed upon a copper radiator, .05 of a radiation length thick. After passing through the radiator foil, the electrons were deflected into a beam dump,

and the photon beam was collimated to 1-inch in diameter and passed through the deuterium target.

The target cell was a vertical cylinder 3-inches in diameter with nickel plated stainless steel walls (.001 in. Stainless Steel, .0005 in. Nickel). The target was of the condensation type and consisted of three such cells. The first was normally filled with liquid deuterium, the second with liquid hydrogen and the third was empty. The intensity of the photon beam was measured by a Secondary Emission Quantameter located behind the target. The device was calibrated several independent ways and the reproducibility of the calibration checked frequently during the course of the experiment. The photo-disintegration reaction was identified by determining the momentum and angle of the recoil protons by means of a 100-in. radius, 90° bend, $n = 0$ magnetic spectrometer which had a solid angle of approximately 1 msr and a momentum acceptance of 1.33 percent for each of three identical scintillation counters placed in the focal plane of the spectrometer. These three momentum defining counters were then put in coincidence with a fourth backing counter, and the rates in the three individual channels as well as their sum were monitored. The accidental coincidence rate was kept to a fraction of a percent of the coincidence rates. Rate dependent corrections were kept completely negligible. Proton detection was performed primarily by ionization loss measurements in the counters. A time-of-flight measurement of the spectrometer particle flux with respect to the r.f. structure of the electron beam verified that the proton signal was uncontaminated.

The experimental procedure was to set the spectrometer momentum and angle for the appropriate gamma ray energy and CM angle. This completely constrains the kinematics of the reaction. The proton yields are then measured as a function of the Bremsstrahlung end-point energy (i.e., the energy of the

accelerator) and a complete proton yield curve is traced out from the photodisintegration threshold to some 100-150 MeV above the photodisintegration threshold where protons associated with pion production begin to appear. The measurement of a complete yield curve ensures that the protons from pion production do not contaminate the photodisintegration sample. One such yield curve is shown in Figure 1. The solid curve is the thick target Bremsstrahlung spectrum⁽⁷⁾ folded with the resolution function of the spectrometer and normalized to the data point at 320 MeV. The protons from the photodisintegration reaction are clearly separated from protons associated with pion production. The fit to the yield curve further shows that the relative shape of the Bremsstrahlung spectrum folded with the resolution function is well understood. In practice, we have measured such yield curves for extreme forward and backward proton angles to verify that there is no contamination of the photodisintegration signal. The intermediate angle points were then measured only at Bremsstrahlung end-point energies corresponding to the plateau of the Bremsstrahlung curve.

In the yield curve shown in Figure 1 the empty target background has been subtracted. This proton background, primarily due to interactions in the walls of the cell, was measured both with a hydrogen cell and with an empty cell. The two background measurements always agreed, thus ensuring that the background did not depend upon whether the target cell was full or empty. These background measurements were made for every photodisintegration data point, and were usually 10-20 percent of the photodisintegration yields.

The photodisintegration cross-sections have been determined by normalizing to electron proton elastic scattering at $E = 1000$ MeV and $q^2 = 8.18F^{-2}$, detecting the recoil proton. We have applied two corrections to this ratio. One is due to the change of the spectrometer acceptance as a function of angle

for a finite target length. For the target used in this experiment this amounts to a maximum correction of 4 percent and was determined experimentally. The second correction is due to the target energy loss of the recoil protons and the resultant effect this has upon determining the effective photon energy interval Δk . This correction varies between 2 percent for forward angles and the highest photon energy, to 25 percent for backward angles and the lowest photon energy. The elastic cross-section has been taken from the form factor fit of T. Janssens et al.⁽⁸⁾

The resultant cross-sections are plotted in Figure 2. For comparison purposes, the recent Bonn and Orsay^(5,6) data are also shown. At 302 and 342 MeV the agreement is good at all angles. For 202 and 254 MeV the present results are all higher than the Bonn and Orsay data, and in particular the shape of the differential cross-section at 222 MeV differs from the earlier measurements.

The measured differential cross-sections in the center of mass system have been fitted to a polynomial of the form $d\sigma/d\Omega = \sum_{i=0}^N a_i \cos^i \theta_{CM}$. The values of the coefficients as well as their errors have been listed in Table I. Small corrections have been made to allow the data to be presented at exactly one photon energy. The statistical accuracy of the data points is generally 1 percent or better. The data were reproducible to within the quoted statistical accuracy over the whole extent of the experiment. The combined effect of the statistical and correction uncertainties is about 1.5 percent. In addition, there is an estimated overall normalization uncertainty of 7 percent.

The plotted cross-sections are determined from the sum of the three momentum channels in the spectrometer. From the separate rates in the three counters it is possible to determine the variation of the cross-section with photon energy. We find no significant difference in the measured cross-section results by using the center counter alone rather than the sum of all three.

Therefore, the measured cross-sections are not significantly dependent upon the experimental resolution. The resolution in photon energy for all three counters is typically 18 MeV at 222 and 254, 20 MeV at 302 and 25 MeV at 342 except for proton CM angles larger than 130° where the resolution becomes larger due to the increased energy loss in the target. The most striking features of the data are the well known peak in the total cross-section at about 260 MeV and the rapid fall off with increasing photon energy. The peak is due to the virtual excitation of the 1236 MeV N^* resonance. The differential cross-section data extend to more forward and backward angles than previous experiments and show a tendency towards leveling off towards forwards and backwards angles. This is particularly observed in the 302 MeV and 342 MeV data.

The most recent and complete calculation of the photodisintegration is the one of Hasselmann⁽⁹⁾. In contrast with earlier calculations, they are in reasonable agreement with the experimental data for the differential cross-section.

A more detailed account of the experiment and comparison with theory will be published elsewhere.

Acknowledgements

We are indebted to J. Grant, L. Boyer and P. Zihlmann for their support during the experiment. We are also indebted to J. Johnson for his help with the construction of the counters and the data analysis.

REFERENCES

1. J. Bernstein, G. Feinberg, and T. D. Lee, Phys. Rev. 139, B1650 (1965).
2. S. Barshay, Phys. Letters 17, 78 (1965).
3. S. Barshay, Phys. Rev. Letters 17, 49 (1966).
4. J. C. Keck and A. V. Tollestrup, Phys. Rev. 101, 360 (1956).
5. R. Kose, W. Paul, K. Stockhorst, and K. H. Kissler, Z. Physik 202, 364 (1967).
6. J. Buon, V. Gracco, J. Lefrancois, P. Lehmann, B. Merkel, and Ph. Roy. Phys. Letters 26B, 595 (1968).
7. R. A. Alvarez, High Energy Physics Laboratory Reprint, HEPL-288 (1961) Stanford University, Stanford, California (Unpublished).
R. A. Early, Stanford Linear Accelerator Center Reprint, SLAC TN-66-15 (1966), Stanford University, Stanford, California (Unpublished).
8. T. Janssen et al., Phys. Rev. 142, 922 (1966).
9. D. Hasselmann, DESY Report. (DESY 68/38 (1968)).

TABLE I

k MeV	N	a_0 ub/sr.	a_1 ub/sr.	a_2 ub/sr.	a_3 ub/sr.	a_4 ub/sr.	a_5 ub/sr.	σ_T ub	χ^2 X/Deg. of Freedom
222	3	5.04 ± .02	1.26 ± .05	-1.23 ± .04	-.70 ± .08	--	--	58.2 ± .3	.812
222	4	5.03 ± .02	1.27 ± .05	-1.05 ± .15	-.71 ± .08	-.21 ± .18	--	58.2 ± .8	.810
222	5	5.03 ± .02	1.16 ± .09	-1.09 ± .15	-.19 ± .38	-.17 ± .18	-.50 ± .36	58.2 ± .8	.775
254	3	5.37 ± .02	1.02 ± .05	-1.33 ± .04	-.47 ± .08	--	--	61.9 ± .3	.960
254	4	5.34 ± .02	1.02 ± .05	-1.07 ± .15	-.48 ± .08	-.30 ± .16	--	61.9 ± .8	.725
254	5	5.34 ± .02	.92 ± .10	-1.07 ± .15	-.02 ± .40	-.31 ± .16	-.42 ± .36	61.9 ± .8	.673
302	3	4.39 ± .02	.76 ± .06	-.93 ± .04	-.26 ± .08	--	--	51.3 ± .3	6.35
302	4	4.52 ± .03	.84 ± .06	-2.06 ± .15	-.42 ± .08	1.26 ± .16	--	51.3 ± .8	.988
302	5	4.53 ± .03	.71 ± .10	-2.15 ± .16	+.18 ± .39	1.37 ± .17	-.55 ± .34	51.3 ± .9	.637
342	3	3.04 ± .02	.35 ± .04	-.64 ± .04	-.007 ± .066	--	--	35.6 ± .3	7.15
342	4	3.13 ± .02	.41 ± .04	-1.52 ± .12	-.14 ± .07	1.07 ± .14	--	35.7 ± .7	1.32
342	5	3.13 ± .02	.44 ± .08	-1.53 ± .12	-.31 ± .31	1.08 ± .14	.17 ± .28	35.7 ± .7	1.34

FIGURE CAPTIONS

Figure 1: Proton yield curve showing photodisintegration threshold at 222 MeV for a proton center-of-mass angle $\theta_{CM} = 20^\circ$. The solid line is a calculated curve from a thick target Bremsstrahlung function with the experimental resolution folded in.

Figure 2: The CM differential cross-sections for four photon energies. The solid lines are a least squares polynomial fit to the data and the least squares coefficients are given in Table I. \triangle represents the Bonn data at 220, 260, 300, and 340 MeV. \square Shows the Orsay data at 220, 255, 302, and 342 MeV. The cross-section at the two last energies were determined by interpolating between the measured values. Typical errors are shown for each energy.

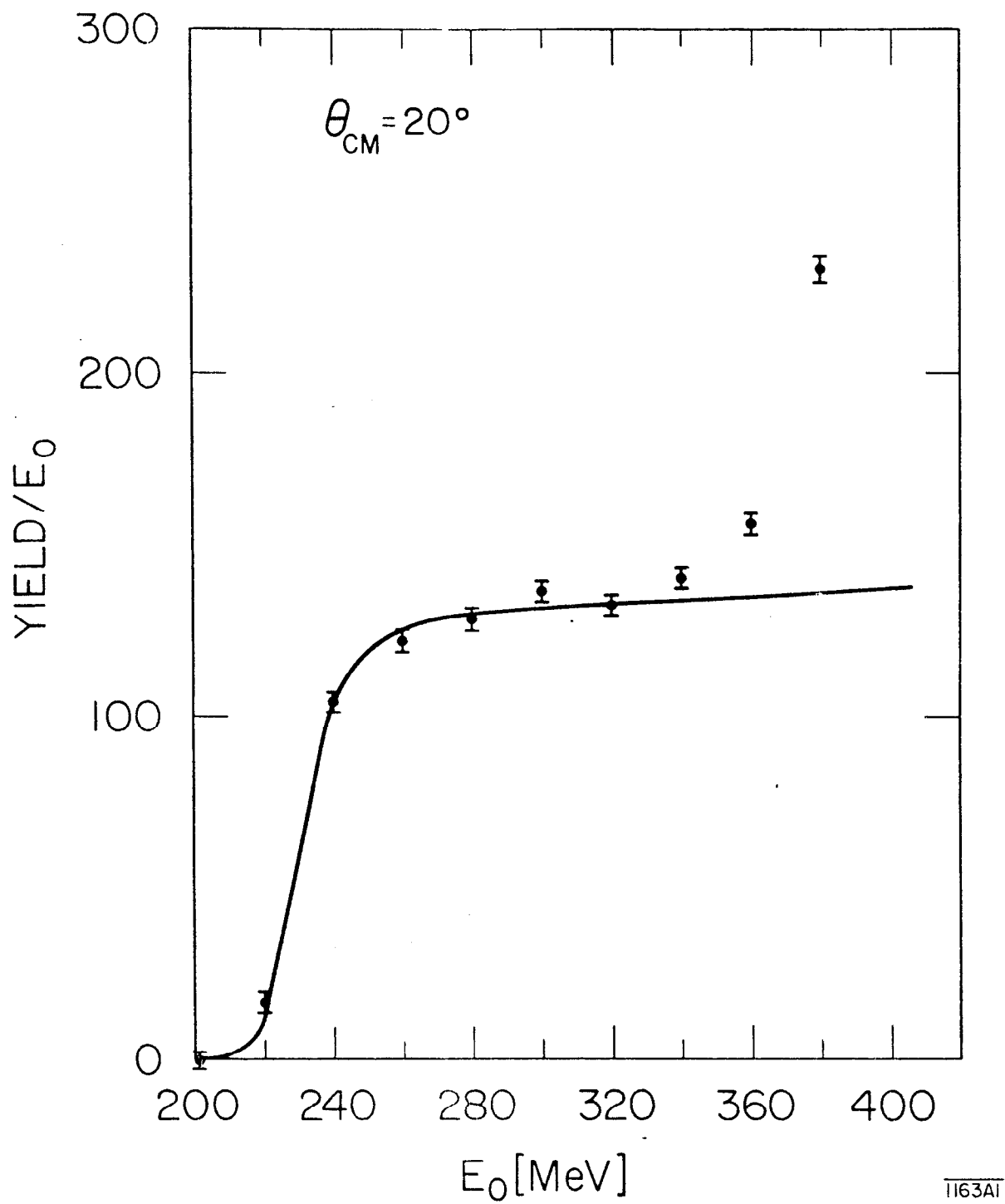
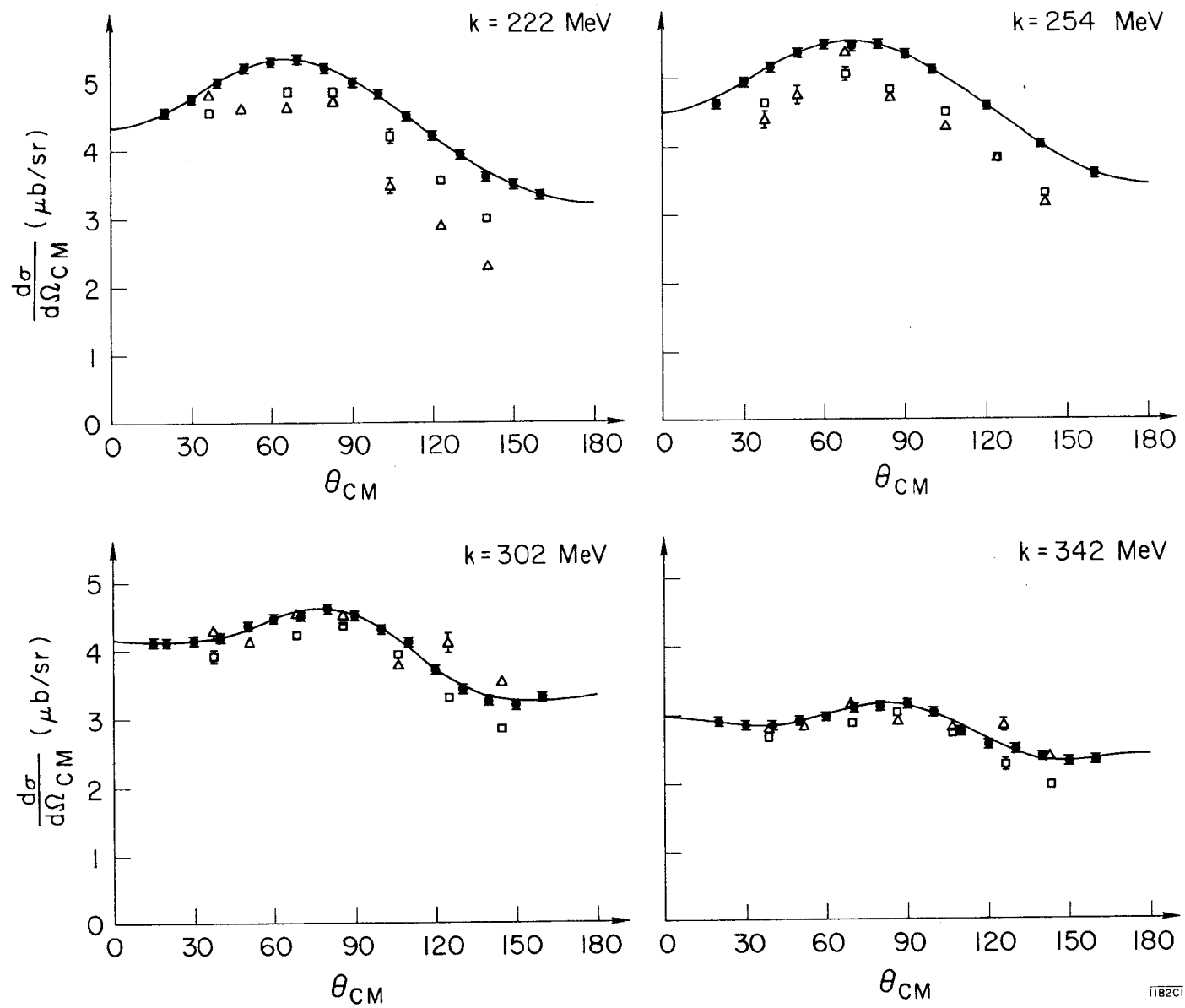


Fig. 1



1182C1

Fig. 2